Dense Regular Packings of Irregular Nonconvex Particles

Joost de Graaf,[1,*] René van Roij,[2] and Marjolein Dijkstra[1,†]

[1]*Soft Condensed Matter, Debye Institute for Nanomaterials Science, Utrecht University, Princetonplein 5, 3584 CC Utrecht, The Netherlands*

[2]*Institute for Theoretical Physics, Utrecht University, Leuvenlaan 4, 3584 CE Utrecht, The Netherlands*

(Received 23 June 2011; revised manuscript received 17 August 2011; published 3 October 2011)

We present a new numerical scheme to study systems of nonconvex, irregular, and punctured particles in an efficient manner. We employ this method to analyze regular packings of odd-shaped bodies, both from a nanoparticle and from a computational geometry perspective. Besides determining close-packed structures for 17 irregular shapes, we confirm several conjectures for the packings of a large set of 142 convex polyhedra and extend upon these. We also prove that we have obtained the densest packing for both rhombicuboctahedra and rhombic enneacontrahedra and we have improved upon the packing of enneagons and truncated tetrahedra.

DOI: 10.1103/PhysRevLett.107.155501 PACS numbers: 61.66.−f, 02.60.−x, 61.46.Df, 82.70.Dd

The synthesis of colloids and nanoparticles has advanced tremendously over the last decade [1–4]. Currently it is not only possible to synthesize spherical particles, but also a wide variety of convex faceted shapes, such as tetrahedra, cubes, and octahedra [1,3]. Perhaps the most remarkable advancement in synthesis techniques is the capability to create with high precision and reproducibility nonconvex, irregular, and even punctured particles, e.g., colloidal caps [4], tetrapods [2], and octapods [5]. Along with the increased availability of complex shapes, there is a concurrent increase in the study of their self-assembly into liquid [6], amorphous [7], and ordered (quasi) crystalline structures [8], as well as their material properties. Interestingly, in studying these dense configurations, materials-science research interfaces with fields as diverse as discrete geometry, number theory, and computer science [9–12].

Predictions obtained from computer simulations on the phase behavior and the self-assembled structures of these particles have been essential in guiding experimental studies and in answering fundamental mathematical questions on the packing of particles. Convex objects such as spheres [6,12] and ellipsoids [7], as well as (semi) regular [9,11,13–18] and space-filling [19] solids have been the subject of intense ongoing investigation. However, ordered structures composed of irregular nonconvex particles have hardly been studied by simulation. Implementing excluded-volume interactions for such systems imposes numerical challenges, because of the complex particle shape and the additional rotational degrees of freedom. Only recently were the first attempts made to study such systems, namely, for superdisks, superballs [20], and bowls [21].

In this Letter, we present a novel composite technique by which we numerically study the dense packings of nonconvex irregular solids, colloids, and nanoparticles. The technique consists of the following elements: the floppy box Monte Carlo method [22] (FBMC), the triangular tessellation method [23] (TT), and the triangle interference detection method [24] (TID). The choice for these individual elements is based on their successful application elsewhere. The FBMC method forms the core of the technique and is an isothermal-isobaric (NPT) ensemble Monte Carlo (MC) simulation, by which crystal structures can be predicted. The hard-particle interaction in this simulation is handled using TT, by which any shape is approximated with triangles, in tandem with TID, by which intersections of triangles are efficiently determined. Two particles overlap whenever there is an intersection between a pair of triangles in the respective TT meshes. To speed up the overlap algorithm and prevent inclusions we employed inscribed- and outscribed-sphere overlap predetection. Interior triangles can be added to a particle to further prevent inclusions, whenever the gap between a particle and its inscribed sphere is too wide. This is allowed because TID models do not have to obey topological constraints [24].

In order to demonstrate the general applicability of this method, we apply our technique to study packings of an enormous set of 142 convex polyhedra and 17 irregular particle shapes, also see the Supplemental Material [25]. This set includes a few models that contain a huge number of triangles, e.g., the colloidal cap, the Stanford bunny, and the hammerhead shark, with 3850, 3756, and 5116 triangles, respectively. All particle models have been generated using particle databases or created to resemble existing nanoparticles and colloids [2,4,5]. Systems of tessellated particles are prepared in a dilute phase. By gradually increasing the reduced pressure we are able to compress the system to a high-density crystalline state. We apply this scheme many times and select the densest packing among these. This packing is allowed to compress further to obtain a maximally compressed state, see Ref. [25] for further details. The method is typically quite fast with simulations taking minutes to hours on a modern

desktop PC [25]. Even for high-triangle models the time scales are accessible, mostly due to the advanced TID routine employed [24]. For the purpose of analyzing nanoparticle systems at lower pressures [5], soft potential terms may be added by introducing point interaction sites distributed over the particle.

It should be noted that the FBMC method is similar to the adaptive shrinking cell (ASC) method of Refs. [14,15], since both allow for a sequential search of configurational space and lattice space using a Metropolis based MC procedure. However, the FBMC method uses a lattice reduction technique [26] to avoid unphysical distortions of the unit cell, whereas the ASC algorithm employs a symmetric strain tensor. In addition, the FBMC method drives the system towards its densest configuration by employing a gradual pressure increase in an NPT-MC simulation scheme, whereas the ASC method drives compression using the negative packing fraction as the basis of its Metropolis acceptance rule. The method of Ref. [27] should also be mentioned, as a different means of determining densest packings. Of the three techniques, the FBMC method has the advantage that it can be used to explore suboptimal packings in accordance with the statistical NPT ensemble at finite pressures. The densest-packed candidate crystal structure need not be thermodynamically stable at all pressures for which the system crystallizes [5,18,19]. However, it goes beyond the scope of this Letter to determine which of the techniques is most suited to achieving densest-packed structures.

To prove the accuracy of our method, we have redetermined the lower bound ϕ_{LB} to the volume fraction of the densest packing both for the 5 Platonic and for the 13 Archimedean solids. We find excellent agreement [25] with Refs. [11,14–17]: the system was typically compressed to within 0.002 of the ϕ_{LB} literature value. The simulations we performed yielded a very narrow distribution of crystal-structure candidates near the closest-packed configuration. The densest of these only required minimal additional compression to achieve the given densest packing fraction value ϕ_{LB}. Moreover, for truncated tetrahedra we have discovered a new crystal structure, a dimer lattice with $\phi_{\mathrm{LB}} = 0.988\ldots$, see Fig. 1 and Ref. [25]. This is not only mathematically interesting [28], but also relevant to the study of nanoparticle systems, since truncated tetrahedra have recently been synthesized [29].

After verifying the accuracy of our technique, we applied our method to study 17 nonconvex (irregular) shapes, some of which even contained holes, thereby going beyond existing studies. Figure 2 shows representations of the shape and predicted crystal structure for 4 different particles, see Ref. [25] for additional information. Such candidate crystal structures can be used in large simulations or theory to determine their stability using, e.g., free-energy calculations. One physical system we considered in more detail is that of the colloidal cap, see Fig. 2(a), which shows

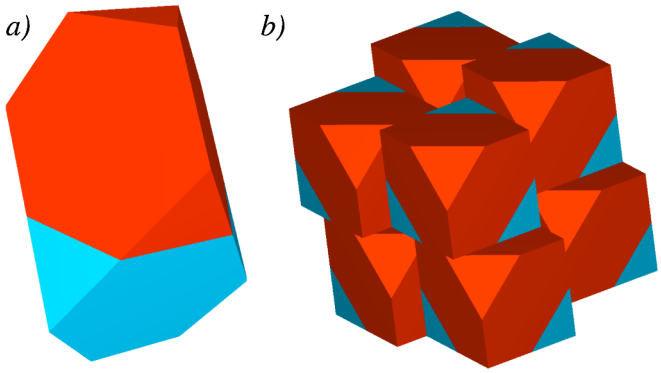

FIG. 1 (color online). The dimer crystal structure for truncated tetrahedra that achieves a packing fraction $\phi_{\mathrm{LB}} = 0.988\ldots$. (a) The dimer formed by two truncated tetrahedra (blue and red; dark and light gray, respectively). (b) A piece of the crystal structure this unit cell generates; only 7 periodic images are shown. The viewpoint is such that the dimers in this crystal are pointing out of the paper, with the top triangle [as given in (a)] facing the reader.

the model that was used. The model is derived from a numerical analysis: the Hamiltonian that describes the bending and in-plane stretching elasticity terms [4,30], which govern the collapse of a shell under an external isotropic pressure, was minimized using surface evolver [31]. The cap that was obtained in this way contains 3850 triangles. We found our model to yield crystal structures similar to the ones that were obtained using a much simpler bowl-shaped model [21]: columnar, braided, and inverse braided phases [25]. Figure 2(b) shows a braided configuration. Support is thus provided for the idea that the simple bowl shape [21] captures the essential shape-related physics of these systems.

Another physical system we studied in greater detail was that of octapod-shaped nanocrystals [5] [Fig. 3(a)]. In Ref. [5] we analyzed the hierarchical self-assembly of these objects into interlocked chains and three dimensional (3D) superstructures by including attractive van der Waals interactions between the octapods. Figure 3 shows an example (simple-cubic) candidate crystal structure obtained by our method for a system of octapods with a soft interaction potential: the centroids of the tips are attracted to each other according to a short-ranged, yet deep square-well interaction. Although simulations on octapods proved technically challenging, we can conclude that such systems may be studied over a range in volume fractions and that the hard-particle overlap can be supplemented with soft interaction potentials to more accurately model the experimental system. By these two physical examples, caps and octapods, we have shown that we can study previously inaccessible nanoparticle and colloid systems, as well as approximate their shape with greater precision, if required.

In the course of our investigation we also obtained several exciting and remarkable results on the packing of

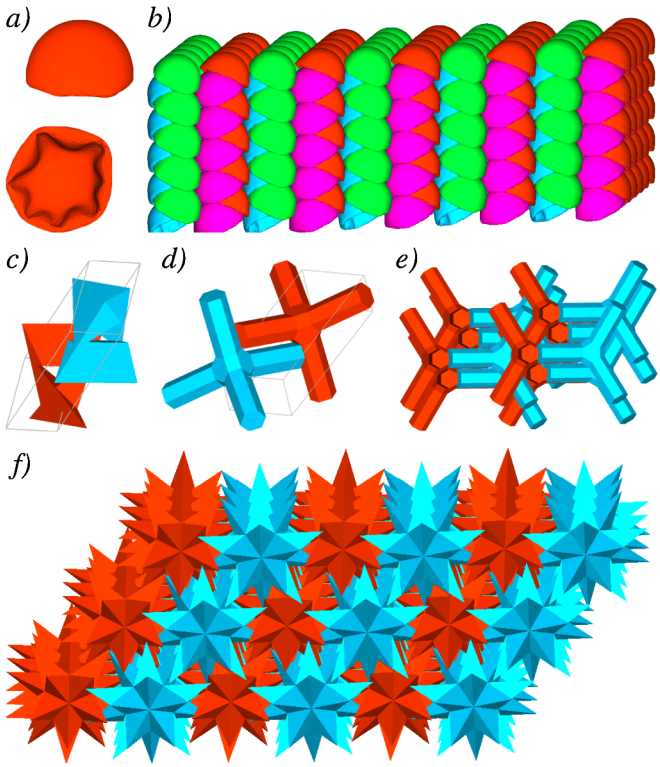

FIG. 2 (color online). Four nonconvex shapes and three of their associated crystal structures. (a) A side and bottom view of the model (3850 triangles) for a colloidal cap. (b) A piece of the double-braided structure formed by these caps. There are four particles in the unit cell, i.e., the caps form a quadrumer, each has been indicated with a different color. (c) The centrosymmetric dimer formed by two Szilassi polyhedra (blue and red; dark and light gray, respectively) that achieves the densest-known packing in relation to its unit cell (gray box). We do not show the crystal this generates, since it is difficult to make out individual particles in it even when they are color coded. (d) A centrosymmetric tetrapod dimer (red, blue) and the associated unit cell (gray box). (e) A piece of the crystal structure formed by this dimer. (f) The densest-known packing for great stellated dodecahedra, again the structure is a dimer lattice as indicated by the red and blue color coding.

faceted particles [25]. (i) We have extended the verification of Ulam's conjecture [32], which states that all convex objects pack denser than spheres, to: the first 8 regular prisms and antiprisms, the 92 Johnson solids, and the 13 Catalan solids [25]. For regular n-prisms and n-antiprisms, where n indicates the number of edges of the bases, the verification of Ulam's conjecture may be further extended to $n = \infty$. For regular prisms this follows from the analysis of regular n-gons [9,10] and the columnar way in which these prisms stack, whereas for antiprisms an outscribed-cylinder estimate for ϕ_{LB} shows that it is sufficient to check up to $n = 7$. (ii) Our results show that there is no clear dependence between the sphericity γ, the ratio of the inscribed- and outscribed-sphere radius, and the densest packing fraction ϕ_{LB} [25]. (iii) We confirmed for 49

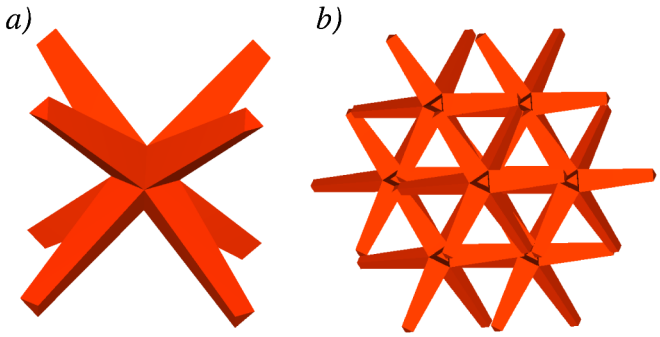

FIG. 3 (color online). A crystal structure obtained for octapod-shaped particles, which have an additional soft interaction term. (a) The model of the octapod used in this simulation. (b) Side view of the candidate crystal structure, which is a simple cubic phase. Note that the octapods touch each other at the tips.

convex centrosymmetric particles that their densest-known lattice packing is a Bravais lattice, in accordance with the conjecture of Ref. [14]. (iv) Our data also support the conjecture [15] that convex, congruent solids without central symmetry do not necessarily pack densest in a Bravais lattice. In general noncentrosymmetric particles do not pack densest in a Bravais lattice, however, there are indications that some do. A possible example is the snub cube [Fig. 4(c)] that achieves $\phi_{\mathrm{LB}} = 0.787\ldots$ for $N = 1$ particle in the unit cell (Bravais lattice). We confirmed this using an extended sample set to achieve a higher numerical accuracy [25]. This may be an indication that central symmetry is not as strong a prerequisite for 3D systems, in contrast with the result for two-dimensional (2D) packings [33]. However, our result constitutes only a possible counterexample, not a full mathematical proof. Nevertheless, the snub cube is not the only particle for which we have observed this [25], e.g., the snub

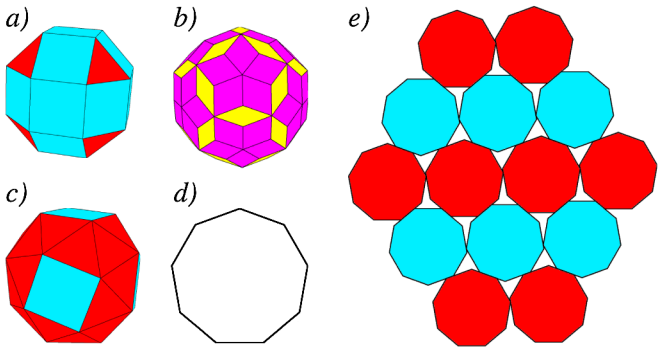

FIG. 4 (color online). Four representations of convex particles and the densest-known packing for enneagons. A rhombicuboctahedron (a) and rhombic enneaconrahedron (b). For both we have proved that its Bravais lattice packs densest. (c) The snub cube, which is not centrally symmetric, yet it achieves its densest-known packing in a Bravais lattice. (d) An enneagon. (e) The centrosymmetric-dimer (blue, red) lattice that achieves the densest packing for enneagons.

dodecahedron and the metabigyrate rhombicosidodecahedron probably achieve their densest packing for $N = 1$. For the snub cube and snub dodecahedron this possibility was already alluded to in Ref. [34]. (v) Many noncentrosymmetric particles, both convex and nonconvex, do form a centrosymmetric compound which achieves the densest regular packing, e.g., truncated tetrahedra [Fig. 1(a)], (anti)prisms ($n < 11$), Szilassi polyhedra [Fig. 2(c)], and tetrapods [Fig. 2(d)], form centrosymmetric dimers and tetrahedra form centrosymmetric quadrumers [17]. (vi) Remarkably, it appears that some noncentrosymmetric particles, e.g., the gyrate rhombicosidodecahedron and the tetrapod, have a noncentrosymmetric $N = 1$ packing and an $N = 2$ centrosymmetric-dimer packing that achieve (nearly) the same packing fraction.

For rhombicuboctahedra [RCH, Fig. 4(a)] and rhombic enneacontrahedra [RECH, Fig. 4(a)] our technique established the densest packing [25]. We found that ϕ_{LB} equals the inscribed-sphere upper bound ϕ_{UB} to the packing fraction [14] within the numerical precision. We subsequently verified this by analytic calculation: for RCH $\phi_{\mathrm{LB}} = \phi_{\mathrm{UB}} = (4/3)(4\sqrt{2} - 5)$ and for RECH $\phi_{\mathrm{LB}} = \phi_{\mathrm{UB}} = 16 - 34/\sqrt{5}$. Here we have redetermined the ϕ_{UB} for the RCH, which was incorrectly listed as $\phi_{\mathrm{UB}} = 1$ in Ref. [14]. Interestingly, we can now invoke the same argument as for spheres [14] and determine two additional upper bounds to the densest packing fraction, based on the largest inscribed RCH and RECH, respectively. By extension of our result for the 9-prism, we also obtained a new 2D packing [Fig. 4(e), Ref. [25]] with $\phi_{\mathrm{LB}} = 0.901\ldots$ for the regular Enneagon [Fig. 4(d)] that surpasses the previously obtained value of $\phi_{\mathrm{LB}} = 0.897\ldots$ [10].

In conclusion, we have shown that regular packings of irregular, nonconvex, and punctured objects may be obtained in a rigorous way by means of our composite technique. The complex problem of the packing of such shapes has been tremendously reduced by the FBMC method and triangulation. We have predicted candidate crystal structures for (faceted) nonconvex and irregular particles, improved upon the literature values for the densest packings of a huge number of solids, and confirmed and extended upon existing conjectures on their densest packing. Moreover, we also prove that we obtained the densest packing of rhombicuboctahedra and rhombic enneacontrahedra. This is remarkable not only because it has historically [12] been exceedingly difficult to prove that the densest packing of objects is indeed achieved for a certain configuration, but also because these particles can now be used to determine new estimates for the upper bound to the maximum packing fraction for other particle shapes. Finally, we also discovered denser packings than previously obtained for noncentrosymmetric enneagons and truncated tetrahedra in centrosymmetric-dimer lattices. In addition, our method can easily be extended to study dense amorphous (granular) and quasicrystalline packings and systems of arbitrarily shaped colloids and nanoparticles with soft interaction potentials in an external field, both in and out of equilibrium. Our method thus opens the way to a more comprehensive study of the material and structure properties than has previously been considered feasible.

M. D. acknowledges financial support by a "Nederlandse Organisatie voor Wetenschappelijk Onderzoek" (NWO) Vici Grant, and R. v. R. by the Utrecht University High Potential Programme.

*j.degraaf1@uu.nl
†m.dijkstra1@uu.nl

[1] Y. Sun and Y. Xia, Science **298**, 2176 (2002).
[2] L. Manna *et al.*, Nature Mater. **2**, 382 (2003).
[3] S. C. Glotzer and M. J. Solomon, Nature Mater. **6**, 557 (2007).
[4] C. Quilliet *et al.*, Eur. Phys. J. E **27**, 13 (2008).
[5] K. Miszta *et al.*, Nature Mater. (in press).
[6] J. D. Bernal and J. Mason, Nature (London) **188**, 910 (1960).
[7] A. Donev *et al.*, Science **303**, 990 (2004).
[8] D. V. Talapin *et al.*, Nature (London) **461**, 964 (2009).
[9] G. Kuperberg and W. Kuperberg, Discrete Comput. Geom. **5**, 389 (1990).
[10] Y. Limon Duparcmeur, A. Gervois, and J. P. Troadec, J. Phys. I (France) **5**, 1539 (1995).
[11] U. Betke and M. Henk, Comput. Geom. **16**, 157 (2000).
[12] T. C. Hales and S. P. Ferguson, Discrete Comput. Geom. **36**, 1 (2006).
[13] A. Haji-Akbari *et al.*, Nature (London) **462**, 773 (2009).
[14] S. Torquato and Y. Jiao, Nature (London) **460**, 876 (2009).
[15] S. Torquato and Y. Jiao, Phys. Rev. E **80**, 041104 (2009).
[16] S. Torquato and Y. Jiao, Phys. Rev. E **81**, 041310 (2010).
[17] E. R. Chen, M. Engel, and S. C. Glotzer, Discrete Comput. Geom. **44**, 253 (2010).
[18] A. Haji-Akbari, M. Engel, and S. C. Glotzer, arXiv:1106.4765v2 [J. Chem. Phys. (to be published)].
[19] U. Agarwal and F. A. Escobedo, Nature Mater. **10**, 230 (2011).
[20] Y. Jiao, F. H. Stillinger, and S. Torquato, Phys. Rev. E **79**, 041309 (2009).
[21] M. Marechal *et al.*, Nano Lett. **10**, 1907 (2010).
[22] L. Filion *et al.*, Phys. Rev. Lett. **103**, 188302 (2009).
[23] J. de Graaf, M. Dijkstra, and R. van Roij, Phys. Rev. E **80**, 051405 (2009).
[24] GAMMA Research Group (UNC), RAPID, http://gamma.cs.unc.edu/OBB/, 1997.
[25] See Supplemental Material at http://link.aps.org/supplemental/10.1103/PhysRevLett.107.155501 for details on the implementation and efficiency of the method and the properties of the 159 particles studied here.
[26] D. Gottwald, G. Kahl, and C. N. Likos, J. Chem. Phys. **122**, 204503 (2005).
[27] S. Gravel and V. Elser, Phys. Rev. E **78**, 036706 (2008).
[28] Y. Jiao and S. Torquato, arXiv:1107.2300v3; P. F. Damasceno, M. Engel, and S. C. Glotzer, arXiv:1109.1323v1.

[29] B. Wiley, T. Herricks, Y. Sun, and Y. Xia, Nano Lett. **4**, 1733 (2004).
[30] N. Tsapis *et al.*, Phys. Rev. Lett. **94**, 018302 (2005).
[31] K. Brakke, Exp. Math. **1**, 141 (1992) [http://www.emis.de/journals/EM/expmath/volumes/1/1.html].
[32] M. Gardner, *The Colossal Book of Mathematics: Classic Puzzles, Paradoxes, and Problems* (W. W. Norton & Company, New York, 2001), 1st ed.
[33] G. F. Tóth, Discrete Comput. Geom. **14**, 1 (1995).
[34] S. Torquato and Y. Jiao, Phys. Rev. E **81**, 049908(E) (2010).